Nature of the Iron–Ligand Bond in Ferrous Low Spin Hemoproteins Studied by Resonance Raman Scattering

T. Kitagawa,* [1a] Y. Kyogoku,[1a] T. Iizuka,[1b] and M. I. Saito[1b]

Contribution from the Institute for Protein Research, Osaka University, Suita, Osaka, Japan, 565, and the Faculty of Engineering Science, Osaka University, Toyonaka, Osaka Japan, 560. *Received August 11, 1975*

Abstract: The resonance Raman spectra of various hemoproteins, newly observed and reexamined by the 488.0- and 514.5-nm excitation lines, were classified into four groups on the basis of the four key bands which may be used to distinguish the oxidation and spin states of the iron ion in myoglobin (Mb) derivatives. This suggests that there are two kinds of ferrous low spin molecules. They may be specified by the binding scheme of the sixth ligand (L) to the heme iron (Fe). Coordination of lone pair electrons to the empty d_{z^2}(Fe) orbital is essential to the Fe–L bonds in ferrous cytochromes (b_5, c, c_3, f, and etc.), while d_π(Fe)–Π(L) interaction is substantially important besides above interaction in the Fe–L bonds in MbNO and some hemoglobin (Hb) derivatives including HbNO, $HbCNC_2H_5$, HbCO, and HbO_2. It is also found that $HbCNC_2H_5$ dissociates into deoxy Hb and CNC_2H_5 on laser illumination. This photodissociation of the Fe–L bond is more or less common to the latter type of the ferrous low spin hemoproteins and is elucidated consistently with Raman results in terms of one electron molecular orbital theory.

From the studies on the resonance Raman scattering of hemoglobin (Hb) derivatives[2-4] it is claimed that the heme irons of HbO_2 and HbCO are in the ferric state. This result favors the Weiss model[5] rather than the Pauling model[6] regarding the binding scheme of the sixth ligand (L) to the heme iron (Fe). Rimai et al.[7] also asserted that both Fe–L bonds in MbO_2 and MbCO are similar to that in MbCN from the observation of similarity in Raman spectra between MbCO (and MbO_2) and MbCN. However, this interpretation of the Raman spectra is not compatible with other physicochemical properties. Magnetic susceptibility measurements have shown that the heme iron is diamagnetic ($S = 0$)[8] in HbO_2 and HbCO but is paramagnetic ($S = \frac{1}{2}$) in MbCN and HbCN irrespective of temperature.[9] The ^{13}C NMR chemical shift of $Hb^{13}CO$[10-12] is much smaller than that of $Mb^{13}CN$,[13] suggesting that the magnetic moment of Fe, which should induce a contact shift for the ^{13}C NMR peaks of the ligand, is negligibly small in HbCO. Furthermore Mossbauer study of Hb derivatives implies that the heme iron of HbCO is in the ferrous low spin state.[14,15]

We have studied the Raman spectra of various hemoproteins[16,17] and their model compounds.[18,19] It was pointed out in our previous paper[20] that there are two types of Raman spectra for low spin cytochromes corresponding to Raman spectra of either Fe^{2+} or Fe^{3+} protoporphyrin IX bisimidazole complexes. Some of the ferrous low spin derivatives show unexpectedly the Fe^{3+} type Raman spectra. To examine further this problem, Raman spectra have been measured in the present study, for various derivatives of myoglobin whose magnetic properties are well known. We identified a few more ferrous low spin derivatives which give rise to the Fe^{3+} type Raman spectra. Since analysis of the EPR spectra of HbNO[21] and MbNO[22] revealed ca. 30% delocalization of the unpaired electron of NO to Fe^{2+}, the similarity between MbNO and MbCN in the Raman spectra cannot be explained by assuming the heme iron of MbNO to be Fe^{3+} as in MbCN. Thus in the present study, we propose a new interpretation of the Raman data to resolve the above inconsistency.

Experimental Section

Sperm whale Mb (Sigma type II) was further purified with a CM-cellulose column just before the measurement of the Raman spectra. MbCN, MbN_3, MbIm (Im = imidazole), MbOCN, and MbF were obtained by adding 50-fold excesses of KCN, NaN_3, and Im and 1000-fold excesses of KOCN and NaF, respectively, to 0.7 mM solutions (0.1 M phosphate buffer) of Mb. MbNO was obtained by the method of Yonetani et al.[22] Human blood Hb was purified according to Drabkin's method.[23] $HbCNC_2H_5$ and HbCO were obtained by adding CNC_2H_5 and by bubbling CO gas, respectively, into the ferrous Hb solution. All derivatives of Hb and Mb were confirmed by visible absorption spectra with the use of a Hitachi-124 recording spectrophotometer. Cytochrome b_5 (cyt-b_5) isolated from rabbit liver by Omura's method,[24] was generously provided by Professor R. Sato (Osaka University). Biscyanide complex of bovine hemin (Sigma type 1, pH 10.8) [$PP(CN)_2$] was reduced by sodium dithionite and its Raman spectrum was measured in a sealed cell to avoid oxidation.

Experimental procedures for the measurements of the Raman spectra of nonphotodissociable derivatives are described elsewhere.[17] The Raman spectra of the photodissociable complexes were measured in the spinning cell (diameter 2 cm, 1800 rpm) kept at about 5 °C by flushing cold nitrogen gas. Under the spinning condition, sample is illuminated by laser light for ca. 10^{-4} s per one turn (0.03 s).

Results

Raman spectra of various derivatives of Mb excited by the 488.0-nm line are shown in Figure 1, where that of cyt-b_5 is also included as a typical ferrous low spin molecule. The Raman lines, which were used as key bands for iron protoporphyrin complexes previously,[20] are designated as bands I–IV. Bands IV and II can be the oxidation and spin state marker of hemoproteins, respectively,[2-4] while band III can be an indicator for out-of-plane location of the heme iron.[25] We note that band I is sensitive to both the oxidation and spin states of the heme iron.

MbCN with the low spin Fe^{3+} ($S = \frac{1}{2}$) and MbIm and MbN_3, which are spin mixtures but predominantly with the low spin Fe^{3+} at room temperature,[9] show a spectral pattern similar to one another. Therefore the identity of the sixth ligand is not essential to the Raman spectra of hemoproteins. The high spin Fe^{3+} derivatives ($S = \frac{5}{2}$) such as MbH_2O, MbF, and MbOCN give the four bands at ~1610, 1561 (with a shoulder around 1545), 1481, and 1371 cm^{-1}, which are close to the frequencies reported for HbF.[26] Deoxy Mb with the high spin Fe^{2+} ($S = 2$) gives bands at 1604, 1557 (with a shoulder at 1544), 1472, and 1355 cm^{-1}. These four bands are also recognized weakly in the Raman spectrum of MbNO, suggesting that MbNO is partly photodissociated into deoxy Mb and NO. It is noteworthy that the four bands of MbNO, with the low spin Fe^{2+} ($S = 0$),[22] appear at obviously different frequencies (1638, 1562, 1503, and 1375 cm^{-1}) from those of ferrous cyt-b_5 (S = 0) (1617, 1538, 1493, and 1361 cm^{-1}). This difference is also noted for HbNO and $HbCNC_2H_5$ ($S = 0$).[8] The Raman spectrum of HbNO[20] is close to that of MbNO.

Figure 2 illustrates the Raman spectra of $HbCNC_2H_5$ with 530.9 nm excitation. Curves I and II were obtained without

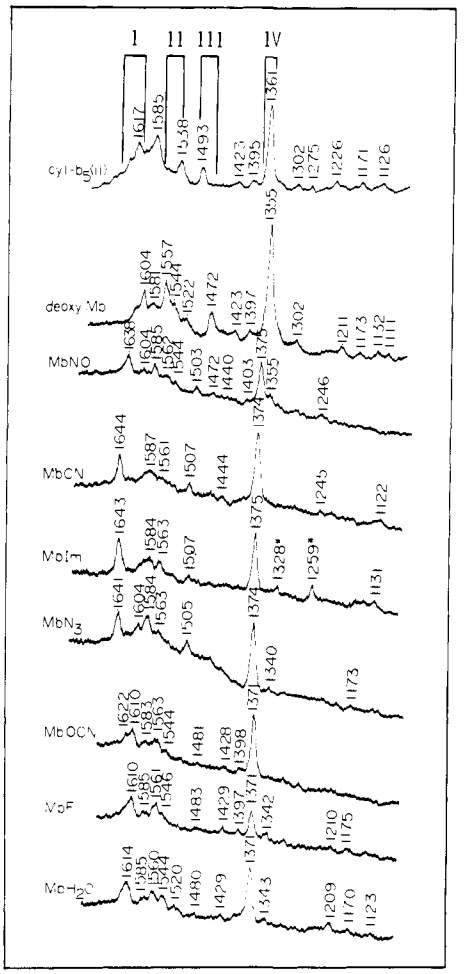

Figure 1. Raman spectra of various derivatives of myoglobin and that of ferrous cytochrome b_5 excited by the 488.0-nm line. I, II, III, and IV correspond to the four key bands used previously to distinguish Fe^{2+} and Fe^{3+} protoporphyrin bisimidazole complexes.[20]

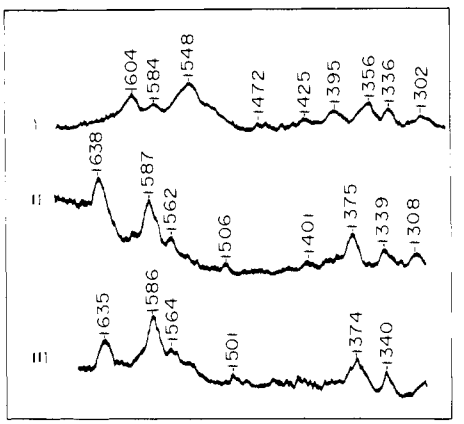

Figure 2. Raman spectra of $HbCNC_2H_5$ in the spinning cell excited by the 530.9-nm line. Curves I and II were obtained without and with spinning the cell, respectively. Curve III was obtained for HbCO with the same experimental conditions (spinning) as those for curve II.

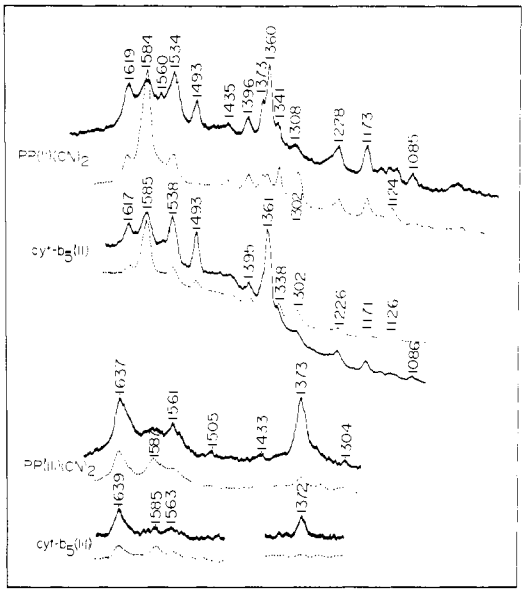

Figure 3. Polarized Raman spectra of dicyanide complex of iron protoporphyrin IX and cytochrome b_5 in ferrous(II) and ferric(III) states. Solid lines and broken lines denote the electric vector of the scattered radiation to be parallel and perpendicular to the electric vector of the incident laser light, respectively.

and with spinning, respectively. For comparison, the Raman spectrum of HbCO, which was reported to be photodissociable by laser illumination,[4] was measured under the same experimental conditions as for $HbCNC_2H_5$. Without spinning the cell, HbCO gave a Raman spectrum almost identical with that of curve I, whereas with spinning the cell, curve III was obtained. The frequencies of the Raman lines for curve I are the same as those for deoxy Hb.[3a] Therefore Figure 2 indicates that $HbCNC_2H_5$ is photodissociated upon laser illumination and that the photodissociation can be apparently retarded by spinning the sample cell.

The four bands of $HbCNC_2H_5$ (1638, 1562, 1506, and 1375 cm^{-1}) are close to those of HbCO and MbNO. Although MbNO (or $HbCNC_2H_5$) and ferrous cyt-b_5 give rise to different types of Raman spectra, the heme irons are coordinated commonly by histidine from one side of the protoporphyrin plane. The other ligand is histidine[27] in cyt-b_5 and NO (or CNC_2H_5) in MbNO (or $HbCNC_2H_5$), respectively. The primary structure of cyt-b_5 is definitely different from that of MbNO (or $HbCNC_2H_5$). To see the effect of the apoprotein the polarized Raman spectra of ferrous and ferric low spin derivatives of protein free protohemes [$PP(CN)_2$] were measured and are compared with those of ferrous and ferric cyt-b_5 in Figure 3. The coincidence of the frequencies and polarization properties of the Raman lines of cyt-b_5 and $PP(CN)_2$ is remarkable in both ferrous and ferric states. Since $PP(CN)_2$ is considered to be planar in both ferrous and ferric states, it seems likely that the frequency difference between ferrous cyt-b_5 (group A) and ferric cyt-b_5 (group C) is caused predominantly by the change of the electron distribution in the heme but not by the difference in the heme-protein interaction or by the distortion of the heme, although the anomalies of Raman spectra of cytochrome c'[28] and horseradish peroxidase[29] were previously attributed to the distortion of the heme.

Figure 4 summarizes the observed frequencies and relative intensities of the four bands (I-IV) for various hemoproteins and protein free hemes newly observed and reexamined by the 488.0-nm (the upper figure) and the 514.5-nm excitation lines (the lower figure). On the basis of the recognizable regularities in the relative intensity and band frequencies of the four bands, the Raman spectra of hemoproteins are classified into four groups (A-D). For excitation at 488.0 nm band IV is always strongest and band III of group D is particularly weak. With the excitation at 514.5 nm band II of group A and band I of group C are relatively intensified. It is noted that the molecules in an individual group show a similar intensity change with the alteration of the wavelength of the excitation line.

Group A includes ferrous low spin ($S = 0$) molecules such as cytochromes and protein free protohemes. Groups B and D

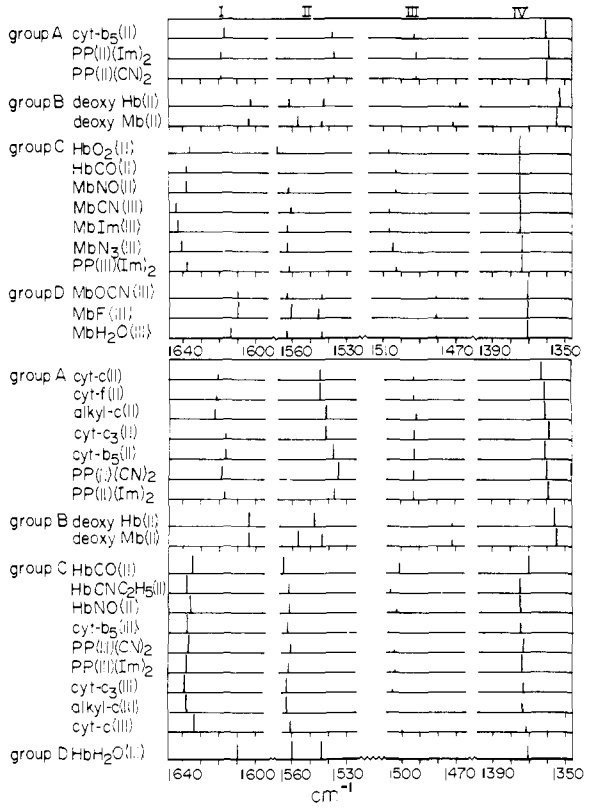

Figure 4. Band intensities and frequencies of the four key bands (I-IV) for the 488.0-nm (upper) and 514.5-nm excitation lines (lower figure). The strongest line is normalized to unity. (II) and (III) denote Fe^{2+} and Fe^{3+}, respectively. Preparation of four cytochromes is described elsewhere.[16,17] Abbreviations: cyt-*c*, cytochrome *c*; cyt-c_3, cytochrome c_3, cyt-*f*, cytochrome *f*; alkyl-*c*, dicarboxymethylmethionylcytochrome *c*; PP(II), ferrous protoporphyrin IX; PP(III), ferric protoporphyrin IX.

cover the ferrous ($S = 2$) and ferric high spin ($S = 5/2$) molecules, respectively. One may note that only the group C includes two kinds of complexes, namely, the low spin Fe^{3+} hemes ($S = 1/2$) and a part of the low spin Fe^{2+} hemes ($S = 0$). This will be discussed in the next section.

High spin molecules show two depolarized components in the frequency region of band II and both are tentatively used as markers. The two components have comparable intensity for the excitation at 514.5 nm, but the component with lower frequency is more intense for the excitation at longer wavelength for HbF.[26] Since the spectral features in this frequency region are independent of the type of heme, the appearance of the two components of band II in the high spin state cannot be ascribed to the vinyl groups of the peripheral substituents. This splitting, however, may possibly be due to the alteration of the selection rule due to the geometrical distortion of the heme group from D_{4h} (groups A and C) to C_{4v} symmetry (groups B and D) on the change of spin states. In the discussion below, attention is focused on the low spin molecules in groups A and C.

Discussion

The Nature of the Fe-L Bond. Band I and bands II, III, and IV were assigned mainly to the methine-bridge[18] and pyrrolic CC and CN[30,31] stretching vibrations, respectively. Their frequencies are influenced by the conjugative interaction of π electrons between the central metal ion and the porphyrin ring.[19] Therefore the Fe-L interaction may affect the conjugative effect between Fe and porphyrin, causing the frequency difference between the molecules in groups A and C.

Since the empty $d_{x^2-y^2}$(Fe) and filled d_{xy}(Fe) orbitals are in the porphyrin plane, they are considered less important for

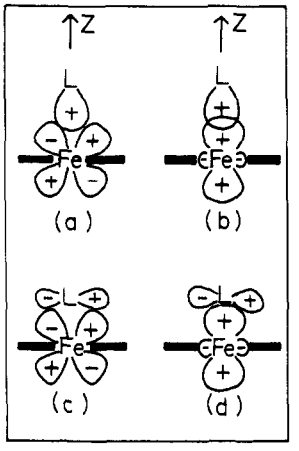

Figure 5. Four types of orbital-overlappings between the iron and axial ligand in low spin hemoproteins. L denotes the sixth axial ligand. (a) The interaction between the d_π (d_{yz} or d_{xz}) orbital of iron and lone pair of L. (b) Coordination of the lone pair electrons of L to the empty d_{z^2}(Fe) orbital. (c) Coordination of d_π(Fe) electrons to the empty (or partially filled) π orbital of L. (d) Coordination of π electrons of L to the empty d_{z^2}(Fe) orbital. The lone pair of L is neglected in (c) and (d). The π orbitals of (c) and (d) can be tilted according to the molecular geometry but even in this case, the present classification can be approximately applied.

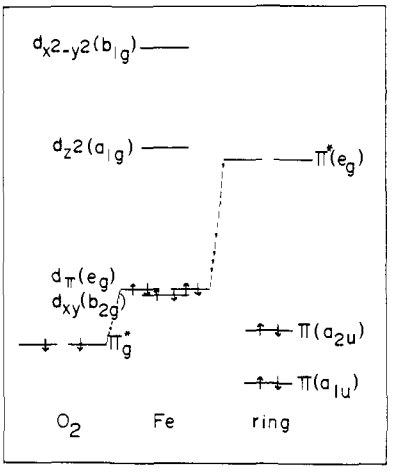

Figure 6. Energy levels of the 3d orbitals of iron (ferrous low spin state), the lowest empty and the two highest filled π orbitals of the porphyrin ring, and the lowest unfilled orbital of the isolated O_2 molecule. The Π_g* denotes a $2p\Pi_g$* molecular orbital of the O_2 molecule. Symmetry species for Fe and porphyrin are designated for the D_{4h} group. The broken line indicates the π-type interaction represented by eq 1.

the interaction with axial ligands. Among four possible cases of the Fe-L interactions, shown schematically in Figure 5, (a) and (d) are of nonbonding type because of symmetry. When the lowest empty orbital of L is fairly high, the lone pair electrons would presumably coordinate to the empty d_{z^2}(Fe) orbital (Figure 5b). It is the case for MbN_3, MbCN, and MbIm (group C, Fe^{3+}). The molecular axis of the N_3^- ion is tilted by 69° from the *z* axis,[32] and the lone pair of the N atom in the sp^2 configuration appears to coordinate to the d_{z^2}(Fe) orbital of the heme iron. Since $C{\equiv}N^-$ takes the sp configuration as in $HC{\equiv}CH$, the coordination of a lone pair is facilitated when the CN axis is parallel to the *z* axis. The lone pair orbital of N(Im) is on the imidazole plane and therefore this molecule is usually bound perpendicularly to the heme plane as seen in the proximal histidyl imidazole.[32]

On the other hand, the lowest unfilled π orbital of the O_2 molecule ($2p\Pi_g$*) lies near the d_π(Fe) orbital,[36] as shown in Figure 6, and the O-O axis is considerably tilted from the *z* axis in the oxygenated picket fence porphyrin.[33] In this case

d_π(Fe)-$\Pi(O_2)$ interaction may contribute significantly to the Fe-L bond.[34,35] This interaction affects the bond strength of the porphyrin ring through the normalized molecular orbital of the e_g species of the D_{4h} group represented by eq 1.

$$\Psi_\pi = c_1 d_\pi(\text{Fe}) + c_2 \Pi^*(\text{ring}) + c_3 \Pi_g^*(O_2) \qquad (1)$$

When the π type interaction is negligible ($c_3 = 0$), the delocalized d_π(Fe) electrons to porphyrin are $3c_2^2$ for group C ferric compounds (c_2^2 from each of three electrons) and $4c_2^2$ for group A ferrous compounds (c_2^2 from each of four electrons). No matter what the value of c_2^2 is, the delocalization of electrons from d_π(Fe) to Π^* (ring) is thus larger for group A ferrous compounds than for group C ferric compounds. Since the Π^*(ring) orbital is of the antibonding type, the larger number of electrons occupying this orbital leads to reduction of the bond strength of porphyrin, and therefore of its stretching force constants. This would explain why the observed Raman frequencies of the four bands (I-IV) are lower in the molecules in group A than those in group C.

The $2p\Pi_g^*$ orbital of an isolated O_2 molecule is presumably split into two components in HbO_2 because of lower symmetry, allowing the lower one be occupied by two electrons.[36] Thus the Fe-O_2 bond might be formed through coordination of the d_π(Fe) electrons to the upper split component of the $2p\Pi_g^*$ orbital. The infrared data for the O-O stretching frequencies of HbO_2 (1107 cm^{-1})[37] and MbO_2 (1103 cm^{-1})[38] are about 30% lower than that of O_2 gas (1555 cm^{-1})[39] and rather close to that of O_2^- in KO_2 (1145 cm^{-1}).[40] It implies that almost one electron is delocalized to O_2 from the d_π(Fe) orbital ($4c_3^2 \approx 1$) and the amount of the d_π(Fe) electrons delocalizable to porphyrin is reduced to three ($4c_1^2 + 4c_2^2 = 3$), which is close to the case of ferric low spin molecules of group C. The EPR study on the HbNO single crystal revealed that the NO axis is tilted by 80° from the z axis,[21] suggesting the existence of Π(L)-d_π(Fe) interaction in HbNO.

Since the lowest empty orbital of CO is relatively higher than that of $\Pi_g^*(O_2)$,[41] c_3^2 is anticipated to be smaller for HbCO than for HbO_2 and therefore c_2^2 is vice versa provided c_1^2 is unaffected. The larger c_2^2 gives rise to the lower vibrational frequencies of porphyrin while the larger c_3^2 leads to the larger frequency shift of the stretching vibration of the ligand on ligation to the heme iron. This is consistent with the observed Raman data[7] that stretching frequencies of porphyrin are slightly higher in HbO_2 than in HbCO and also with the infrared data that the C-O stretching frequencies in MbCO (1944 cm^{-1})[38] and HbCO (1951 cm^{-1})[42] are 10% lower than that of CO gas (2145 cm^{-1})[39] but 30% lower for the O-O stretching frequencies described before.

It must be emphasized that the Fe^{3+}-CN^- bond is completely different from the Fe-O_2 (or Fe^{3+}-O_2^-) bond. The former is of the d_{z^2}(Fe)-lone pair type with $c_3^2 = 0$ whereas the latter is the d_π(Fe)-Π(L) type with larger c_3^2. The Raman oxidation state marker indicates presumably the effective number of electrons delocalized to the Π^*(ring) orbital and not the actual electric charge on the Fe ion.

Photodissociation of the Sixth Ligand. $HbCNC_2H_5$ showed photodissociation upon the laser illumination (Figure 2) and MbNO did partly (Figure 1). The sixth ligands of ferrous molecules in group C are more or less photodissociable for the illumination of light at the Soret band.[43] The present consideration of the π type molecular orbital is also consistent with the observed photodissociation. A schematic energy level diagram of the π type molecular orbitals is shown in Figure 7, where the relative positions of the energy levels are tentative and a single level can contain four electrons due to its degeneracy.

As the first step in the formation of the molecular orbital, we assume the existence of bonding (ϕ_a) and antibonding (ϕ_a^*) orbitals which arise from the d_π(Fe) and $\Pi_g^*(O_2)$ orbitals

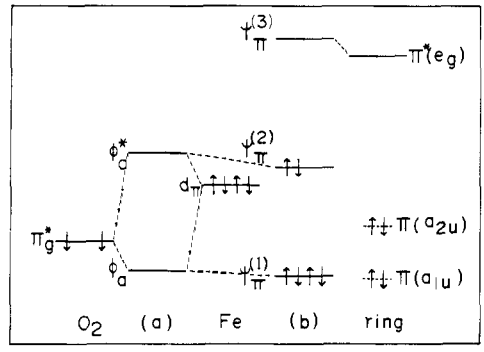

Figure 7. A schematic diagram of the energy levels of the π type molecular orbitals: (a) the presumptive bonding (ϕ_a) and antibonding (ϕ_a^*) orbitals formed from the d_π(Fe) and $\Pi_g^*(O_2)$ orbitals, (b) three levels of the π type molecular orbitals represented by eq 1. When ϕ_a^* is much higher than Π^*(ring), $\Psi_\pi^{(2)}$ should be connected with Π^*(ring). The $\Pi_g^*(O_2)$ is regarded as a degenerate orbital in this figure but it may possibly be split into two components and two electrons may occupy the lower one.[36] This does not alter the present conclusion.

(Figure 7a). We then assume these levels are perturbed through interaction with the Π^*(ring) orbital, resulting in three levels represented as $\Psi_\pi^{(1)}$, $\Psi_\pi^{(2)}$, and $\Psi_\pi^{(3)}$ (Figure 7b). The main effect of the latter interaction is considered to be mixing of two nearest orbitals, that is Π^*(ring) and ϕ_a^*, although the degree of mixing depends upon the energy difference of the two orbitals. As there are six electrons (two from $\Pi_g^*(O_2)$ and four from d_π(Fe)) for HbO_2 and four electrons for HbCO, they would fully occupy the orbital with the lowest energy $\Psi_\pi^{(1)}$ and partly the next lowest $\Psi_\pi^{(2)}$. On the other hand, it is assumed that an electron is excited from Π(ring)(a_{1u}) or Π(ring)(a_{2u}) to Π^*(ring)(e_g) on the illumination of light at the Soret or Q band, respectively.[36] These electronic excitations would be actually to $\Psi_\pi^{(3)}$ when Π^*(ring) is much higher than ϕ_a^* and to $\Psi_\pi^{(2)}$ when Π^*(ring) is lower than ϕ_a^*. In any way, the electron is excited by light to the level which contains ϕ_a^* character considerably. The ϕ_a^* orbital is antibonding with regard to the Fe-L bond. Accordingly the electronic excitation at the porphyrin ring by the illumination of light at the Soret or Q band leads to the dissociation of the sixth ligand of the heme iron, more readily than those systems where the $\Psi_\pi^{(2)}$ (or $\Psi_\pi^{(3)}$) is unoccupied. The difference in photodissociability among HbCO, HbO_2, $HbCNC_2H_5$, HbNO, and MbNO is presumably due to difference in the degree of ϕ_a^* character for the upper level as well as of simultaneous contribution of a Figure 5b type interaction.

In conclusion, the Raman spectra can be used to distinguish two types of Fe-L bonds in ferrous low spin hemoproteins. The sixth internal ligands (methionine, histidine, or lysine) in cytochromes are bound to the heme iron through the d_{z^2}(Fe)-lone pair interaction while the external ligands such as NO, CO, O_2, or alkyl isocyanide in their Hb and Mb complexes which are more or less photodissociable, are bound mainly through the d_π(Fe)-Π(L) interaction.

Acknowledgment. The authors wish to express their gratitude to Professor T. Miyazawa, Tokyo University, and Professor J. Otsuka, Osaka University, for the stimulating discussion. They are also indebted to Professor R. Sato, Osaka University, and to Professor H. Ishimura, Keio University, for the courtesy of providing us with cytochrome b_5 and ethyl isocyanide, respectively. This work was partly supported by grants from the Ministry of Education of Japan and from Mishima Memorial Fund.

References and Notes

(1) (a) Institute of Protein Research; (b) Faculty of Engineering Science.
(2) T. Yamamoto, G. Palmer, D. Gill, I. T. Salmeen, and L. Rimai, *J. Biol. Chem.*,

248, 5211 (1973).
(3) (a) H. Brunner and H. Sussner, *Biochim. Biophys. Acta*, **310**, 20 (1973); (b) H. Brunner, A. Mayer, and H. Sussner, *J. Mol. Biol.*, **70**, 153 (1972).
(4) T. G. Spiro and T. C. Strekas, *J. Am. Chem. Soc.*, **96**, 338 (1974).
(5) J. J. Weiss, *Nature (London)*, **202**, 83 (1964).
(6) L. Pauling, *Nature (London)*, **203**, 182 (1964).
(7) L. Rimai, I. Salmeen, and D. H. Petering, *Biochemistry*, **14**, 378 (1975).
(8) L. Pauling and C. D. Coryell, *Proc. Natl. Acad. Sci. U.S.A.*, **22**, 210 (1936).
(9) T. Iizuka and M. Kotani, *Biochim. Biophys. Acta*, **181**, 275 (1969); **194**, 351 (1969).
(10) F. Conti and M. Paci, *FEBS Lett.*, **17**, 149 (1971).
(11) R. B. Moon and J. H. Richards, *J. Am. Chem. Soc.*, **94**, 5093 (1972).
(12) P. J. Vergamini, N. A. Matwiyoff, R. C. Wohl, and T. Bradley, *Biochem. Biophys. Res. Commun.*, **55**, 453 (1973).
(13) I. Morishima, T. Inubushi, T. Yonezawa, and T. Iizuka, to be submitted for publication.
(14) G. Lang and W. Marshall, *Proc. Phys. Soc., London*, **87**, 3 (1966).
(15) G. Lang, *J. Appl. Phys.*, **38**, 915 (1967).
(16) M. I. Saito, T. Kitagawa, T. Iizuka, and Y. Kyogoku, *FEBS Lett.*, **50**, 233 (1975).
(17) T. Kitagawa, Y. Kyogoku, T. Iizuka, M. I. Saito, and T. Yamanaka, *J. Biochem.*, **78**, 719 (1975).
(18) T. Kitagawa, H. Ogoshi, E. Watanabe, and Z. Yoshida, *Chem. Phys. Lett.*, **30**, 451 (1975).
(19) T. Kitagawa, H. Ogoshi, E. Watanabe, and Z. Yoshida, *J. Phys. Chem.*, **80**, 1181, (1976).
(20) T. Kitagawa, Y. Kyogoku, T. Iizuka, and M. I. Saito, *Chem. Lett.*, 849 (1975).
(21) J. C. Chien, *J. Chem. Phys.*, **51**, 4220 (1969).
(22) T. Yonetani, H. Yamamoto, J. E. Erman, J. S. Leigh, Jr., and G. H. Reed, *J. Biol. Chem.*, **247**, 2447 (1972).
(23) D. L. Drabkin, *J. Biol. Chem.*, **164**, 703 (1946).
(24) T. Omura and S. Takesue, *J. Biochem.*, **67**, 249 (1970).
(25) A. L. Verma and H. J. Bernstein, *J. Raman Spectrosc.*, **2**, 163 (1974).
(26) T. C. Strekas, A. J. Packer, and T. G. Spiro, *J. Raman Spectrosc.*, **1**, 197 (1973).
(27) F. S. Mathews, M. Levine, and P. Argos, *J. Mol. Biol.*, **64**, 449 (1972).
(28) T. C. Strekas and T. G. Spiro, *Biochim. Biophys. Acta*, **351**, 237 (1974).
(29) G. Rakshit and T. G. Spiro, *Biochemistry*, **13**, 5317 (1974).
(30) P. Stein, J. M. Burke, and T. G. Spiro, *J. Am. Chem. Soc.*, **97**, 2304 (1975).
(31) M. Abe, T. Kitagawa, and Y. Kyogoku, *Chem Lett.*, 249 (1976).
(32) L. Stryer, J. C. Kendrew, and H. C. Watson, *J. Mol. Biol.*, **8**, 96 (1964).
(33) J. P. Collman, R. R. Gagne, C. A. Reed, T. R. Halbert, G. Lang, and W. T. Robinson, *J. Am. Chem. Soc.*, **97**, 1427 (1975).
(34) Y. Seno, J. Otsuka, O. Matsuoka, and N. Fuchikami, *J. Phys. Soc. Jpn.*, **33**, 1645 (1972).
(35) J. Otsuka, M. Matsuoka, N. Fuchikami, and Y. Seno, *J. Phys. Soc. Jpn.*, **35**, 854 (1973).
(36) M. Zerner, M. Gouterman, and H. Kobayashi, *Theor. Chim. Acta*, **6**, 363 (1966) (from Figure 2 case VII).
(37) C. H. Barlow, J. C. Maxwell, W. J. Wallace, and W. S. Caughey, *Biochem. Biophys. Res. Commun.*, **55**, 91 (1973).
(38) J. C. Maxwell, J. A. Volpe, C. H. Barlow, and W. S. Caughey, *Biochem. Biophys. Res. Commun.*, **58**, 166 (1974).
(39) G. Herzberg, "Spectra of Diatomic Molecules", Van Nostrand Princeton, N.J., 1965, p 62.
(40) H. Siebert, "Schwingungsspektroskopie in der Anorganischen Chemie", Springer Verlag, Berlin, 1966, pp 40, 51.
(41) See Figures 5 and 6 of ref 36.
(42) J. O. Alben and W. S. Caughey, *Biochemistry*, **7**, 175 (1968).
(43) T. Iizuka, H. Yamamoto, M. Kotani, and T. Yonetani, *Biochim. Biophys. Acta*, **263**, 830 (1972).

Tetrakis(methyl isocyanide)palladium(II) Tetrakis(7,7,8,8-tetracyano-*p*-quinodimethane), $[Pd(CNMe)_4](TCNQ)_4 \cdot 2MeCN$: Synthesis, Structure, and Physical Properties

Stephen Z. Goldberg,[1a] Richard Eisenberg,*[1a] Joel S. Miller,*[1b] and Arthur J. Epstein[1b]

Contribution from the Department of Chemistry, University of Rochester, Rochester, New York 14627, and Xerox Corporation, Webster Research Center, Webster, New York 14580. *Received July 28, 1975*

Abstract: The title compound has been synthesized from the reaction of $[Pd(CNMe)_4](PF_6)_2$, LiTCNQ, and TCNQ in acetonitrile. Its crystal and molecular structure have been determined from three-dimensional x-ray data obtained by counter techniques. The compound crystallizes in the triclinic space group $P\bar{1}$ with one formula unit/unit cell. Cell dimensions are: a = 7.730 (2), b = 14.978 (7), c = 14.389 (4) Å; α = 65.08 (2), β = 81.29 (2), γ = 73.46 (2)°. The conventional R factors (refinement on F) at convergence for 2266 reflections with $F^2 \geq 3\sigma(F^2)$ and $2\theta \leq 45°$ are 0.0459 and 0.0472. The molecular parameters of the two crystallographically independent TCNQ moieties are equivalent. The crystal structure is such that the TCNQ's stack to give tetrameric groups with interplanar distances of 3.29 and 3.32 Å between molecules in the tetramer. At the junction between tetramers the two independent interplanar ring-ring distances are 3.15 and 3.69 Å. The $[Pd(CNMe)_4]^{2+}$ ion has the expected square planar coordination sphere. There are no stacking interactions between the cation and the TCNQ system. Infrared and reflectance spectra are reported, as are magnetic measurements. Conductivity measurements have been made on both pressed pellet and single-crystal samples. The interpretation of the conductivity data is complicated by the triclinic nature of the crystal cell; however, the results are consistent with a quasi-two-dimensional semiconductor behavior.

An active area of recent research has been the synthesis and characterization of new materials which as solids exhibit anisotropic electrical and magnetic properties, and in particular unidirectional metallic behavior. Although limited in number, materials of this latter type, which are called one-dimensional (1-D) metals, span both organic and inorganic chemistry. To date, the most successful organic systems in this area have been based on the anion of 7,7,8,8-tetracyano-*p*-quinodimethane, TCNQ,[2-5] while the best inorganic systems have been developed around the tetracyanoplatinate anion, $Pt(CN)_4^{2-}$.[2,3,6-8] It is now well established that partial oxidation of potassium tetracyanoplatinate(II) with bromine or chlorine leads to the formation of a lustrous, homogeneous material of stoichiometry $K_2Pt(CN)_4X_{0.3}(H_2O)_3$ which has a partially filled electron energy band arising from the overlap of orbitals comprised mainly of platinum d_{z^2} functions.[2,3,6-8] Similarly, the reaction of tetrathiafulvalene, TTF, with TCNQ results in the formation of the charge transfer salt (TTF)(TCNQ) which possesses partially filled electron energy bands arising from the overlap of π molecular orbitals on the segregated stacks of donor and acceptor molecules.[2-5] The structural arrangement in both of these systems which allows band formation involves the